Archives available at journals.mriindia.com

International Journal of Advanced Scientific Research and Engineering Trends

ISSN: 2456-0774

Volume 10 Issue 05, 2026

Substituent and Structural Determinants in the Chromium(VI) Oxidation of Substituted Mandelic Acids: Taft Correlation, Decarboxylation Pathways, and Mechanistic Evolution Across PCC, PDC, QDC, and TBAD

[1]Ashutosh Sharma, [2]Y. K. Mishra, [3]B. K. Dangarh

[1]Research Centre, PMCOE Govt Arts and Science College, Ratlam, Madhya Pradesh 457001, India

[2]PMCOE Govt Arts and Science College, Ratlam, Madhya Pradesh 457001, India

[3]Department of Chemistry, PMCOE Swami Vivekanand Govt PG College, Neemuch, Madhya Pradesh 458441, India

[1]ashutoshdhand24@gmail.com, [2]yashwantmishra265@gmail.com, [3]bkdangarh11@gmail.com

Peer Review Information

Submission: 19 April 2026
Revision: 05 May 2026
Acceptance: 23 May 2026

Keywords

Chromium(VI) oxidation, Mandelic acid derivatives, Taft correlation analysis, Electronic substituent effects, Oxidative decarboxylation, Chromate ester mechanism, Reaction kinetics, α-Hydroxy acid oxidation.

Abstract

The chromium(VI) oxidation of mandelic acid derivatives provides a sensitive platform for probing how substrate electronics and oxidant structure cooperatively govern reaction pathways. In this study, mandelic acid and a series of para-substituted derivatives (p-NO_2, p-Cl, H, p-CH_3, p-OCH_3) were oxidized using four chromium(VI) reagents, pyridinium chlorochromate (PCC), pyridinium dichromate (PDC), quinolinium dichromate (QDC), and tetrabutylammonium dichromate (TBAD), under comparable acidic and solvent conditions. Electronic and structural effects were systematically examined through pseudo–first-order kinetics, Taft σ* correlations, stoichiometric Cr(VI) consumption, product characterization via 2,4-dinitrophenylhydrazone derivatives, and qualitative CO_2 evolution studies.

Taft correlations reveal a pronounced increase in substituent sensitivity across the oxidant series, with low ρ values for PCC (ρ ≈ 0.8), moderate values for PDC, and large positive slopes for QDC (ρ ≈ 1.86) and TBAD (ρ ≈ 2.11). These tendencies reveal that there is a progressive rise in electron deficiency at the α-carbon in the transition state, which is in line with the changing dominance from weakly associated chromate ester pathways in PCC to increasingly substrate–chromium interactive pathways in QDC and TBAD. PCC predominantly effects two-electron oxidation to α-keto acids, whereas QDC and TBAD promote oxidative decarboxylation under electronically favorable conditions, reflected in higher effective Cr(VI) consumption ratios. The identities of the products were confirmed by the 2,4-dinitrophenylhydrazone derivatives characterized by melting point comparison. All of these findings show a distinct mechanistic order of Cr(VI) oxidants, which are both oxidant architecture- and substrate electronic effect-dependent. The results indicate that oxidative decarboxylation becomes competitive when significant transition-state polarization and effective substrate–chromium interaction are present. This article offers a single electronic-mechanistic model on the Cr(VI) oxidations of α-Hydroxy acids.

Introduction

The oxidation of mandelic acid and its para-substituted derivatives by chromium(VI) oxidants gives one of the most structurally informative systems in the explanation of any electronic effects on redox reactions at saturated centres of carbon. Unlike simple aliphatic α-hydroxy acids, mandelic acids contain an aromatic ring directly bonded to the reactive α-carbon. The electronic nature of substituents on the aromatic ring modulates electron density at the α-carbon due to both inductive and resonance interactions and hence, exercise effective control over the rate and direction of oxidation. Substituted mandelic acids provide an informative platform for linear free-energy correlation analysis because substituent-induced electronic effects can be transmitted efficiently to the reactive α-carbon center. Although para-substituted aromatic systems are traditionally analyzed using Hammett σ constants, the present work employs Taft σ* parameters primarily to emphasize inductive contributions to transition-state stabilization at the saturated α-carbon adjacent to the hydroxyl and carboxyl functionalities. Since resonance effects may still contribute, particularly for strongly donating or withdrawing para substituents, the present correlations should be interpreted as predominantly inductive trends rather than purely resonance-independent relationships[1,2]. Though the Taft method was developed in the context of investigating the hydrolysis of ester hydrolysis and nucleophilic reactions at saturated carbon centers, it has also been found useful in studying electron demand in redox reactions with electron withdrawal/donation effects on the transition-state stability[3,4,5]. Although chromium(VI) oxidants have a long history, in organic chemistry, they still provide a complexity in mechanisms long since they were used as classical stoichiometric oxidants. They are mechanistically diverse because Cr(VI) can take on a large number of different reactive conformations, because these different forms are sensitive to protonation, and because the pre-association geometries can be diverse when the substrates have bidentate coordination sites-as the mandelic acids do. Both α-hydroxy and carboxyl groups of mandelic acid are capable of coordinating to chromium so that five- or six-membered cyclic chromate esters are plausible, which may alter the balance between simple oxidation and decarboxylative pathways. [6,7]. Less strongly organized chromate ester pathways generally favor formation of the corresponding α-keto acid without extensive oxidative decarboxylation, whereas more tightly associated substrate–chromium interactions may facilitate competing decarboxylative processes. Past work on Cr(VI) oxidations has tended to focus on a single oxidant or on an unmodified substrate, so little has been done to properly understand the combined effect of substrate electronic structure and oxidant architecture[8-11]. Chromium(VI) oxidations of α-hydroxy acids are widely accepted to proceed through chromate ester intermediates, followed by rate-determining C–H bond cleavage or rearrangement. Numerous kinetic studies have demonstrated that highly negative ΔS‡ values and saturation kinetics are characteristic of cyclic inner-sphere transition states, whereas weak substituent sensitivity and linear rate laws are associated with outer-sphere pathways. The present study situates PCC, PDC, QDC and TBAD within this established mechanistic framework. The series of chromium (VI) oxidants used in this paper, which includes: PCC, PDC, QDC and TBAD, forms the continuum of rising lipophilicity, falling solvation, and rising pre-association probability with substrate. The most polar and, by far, the most strongly solvated, PCC can be active through mechanisms where substrate coordination is brief or low[12]. PDC demonstrates a somewhat improved ability to associate, and QDC and TBAD with their larger organic counter-ions favour a far stronger approach and organisation of substrate around the chromium centre[13,14]. These differences are especially pronounced in the case of an oxidation pathway in which electron-deficient transition states are involved. Oxidative decarboxylation requires stabilization of developing electron deficiency at the α-carbon during C–C bond cleavage [15]. This stabilization is effected by electron-withdrawing substituents, and inhibited by electron-donating substituents. When the oxidant promotes a highly organized and polarized transition state, the electronic impacts of substituents are still more evident[16]. Therefore, the reaction pathway is determined by the interaction of substrate electronics and oxidant mechanistic character. The current study seeks to offer a mechanistic, rigorous and electronic level insight on the effect of mandelic acid substituents on chromium(VI) oxidative processes. In order to accomplish this, multi-component approach was taken. This was done by first establishing pseudo-first-order rate constants of substituted mandelic acids with each of the four oxidants under the same acidic and solvent conditions. Observed rate constants were correlated with Taft σ* constants. Linear free energy relationships represent a direct

assessment of how much substituent inductive effects have an impact on the transition state. Large r values are indicative of a high degree of electronic sensitivity and charge development at the α-carbon, and small r values provide an indication of small electronic effect and an outer-sphere transition state. Second, stoichiometric ratios of consumption of Cr(VI) versus oxidation of substrates were calculated using representative substrates. Mandelic acids may be oxidized to benzoylformic acid, or can oxidatively decarboxylate to benzaldehydes. These routes vary in the number of electrons and the observed stoichiometry hence a mechanistic fingerprint. Reactions that produce the α-keto acid involve net two-electron oxidation at the substrate level, whereas oxidative decarboxylation requires additional electron equivalents, reflected experimentally in higher Cr(VI) consumption ratios. The relative ability of the oxidant to mediate complete decarboxylation and the electronic predisposition of the substrate to such decarboxylation, therefore, becomes apparent through a stoichiometric analysis. Third, the identification of the products was performed by the preparation and melting point determination of 2,4-dinitrophenylhydrazones, which is one of the traditional yet very useful methods used in aldehyde and ketone identification. Benzaldehydes hydrazones have melting points that are very distinctly different to the melting point of hydrazones of benzoylformic acid or other substituted benzaldehydes, and the products can be assigned with reasonable qualitative confidence through comparison with reported derivative melting points. Although modern spectroscopic techniques such as NMR or GC–MS would provide more definitive structural confirmation, the DNPH derivative approach remains useful for distinguishing aldehydic and α-keto products in comparative mechanistic studies.

Also, the experiments of CO_2 evolution were also conducted to verify oxidative decarboxylation where it was suspected. A combination of these analytical methods permits one to develop a consistent mechanistic model, which correlates substituent electronics, oxidant structure, and transition -state architecture. The mandelic acid series, as will be demonstrated in this paper, demonstrates mechanistic behaviours that cannot be determined by kinetic studies per se. Specifically, the electronic substituent effects can provide a strong insight into the reasons why TBAD and QDC are always known to favor cyclic, inner-sphere reactions whereas PCC does not behave similarly, although they all have the same chromium oxidation state. Similarly, stoichiometric and product studies demonstrate why electron-withdrawing substituents readily cause decarboxylation over the electron-donating moieties, and why TBAD stabilizes decarboxylating reactions much more effectively than PDC.

Experimental Study

1. Chemicals and Substrate Preparation

All substituted mandelic acids used in this work, p-nitromandelic acid, p-chloromandelic acid, mandelic acid (unsubstituted), p-methylmandelic acid, and p-methoxymandelic acid, were obtained from Sigma-Aldrich in high purity. Each crystalline substrate was dried under reduced pressure for several hours prior to use to eliminate adsorbed moisture. The purity of substituted derivatives was verified by melting point checks against reported literature values[17-20], ensuring the absence of residual starting materials from synthetic preparation.

Chromium(VI) oxidants were handled with particular care due to their known toxicity. Pyridinium chlorochromate (PCC), pyridinium dichromate (PDC), quinolinium dichromate (QDC), and tetrabutylammonium dichromate (TBAD) were either procured commercially or synthesized freshly by standard metathesis from sodium dichromate and the appropriate organic cation salt. The oxidants had sharp melting or decomposition ranges which validated the lack of mixed-chromate contaminants. The fact that QDC and TBAD are highly sensitive to moisture implies that they were stored in amber glass vials on silica gel and consumed within two weeks after preparation. All the solvents (glacial acetic acid, dimethyl sulfoxide (DMSO), and distilled water) were of analytical grade. QDC and TBAD reactions were done in 30% (v/v) DMSO–water and PCC and PDC reactions were done in 30% v/v acetic acid -water to ensure consistency with solubilities of derivatives reported solubility, reported with substituted mandelic acids[21-25]. The acidity (0.10 M H^+) was maintained constant for each oxidant system using standardized acid solutions. Acidity was maintained at 0.10 M total proton concentration; in DMSO–water systems this was adjusted using perchloric acid, whereas in acetic acid–water systems the medium acidity was governed by added mineral acid. The choice of solvent will be favorable with the highest possible solubility and reduced aggregation or precipitation of more hydrophobic oxidants. The use of two solvent systems was necessitated by solubility and aggregation characteristics of the oxidants. PCC and PDC exhibited optimal solubility and kinetic stability in 30% (v/v) acetic acid–water, whereas QDC and TBAD,

owing to their increased lipophilicity and reduced solvation, required 30% (v/v) DMSO–water for homogeneous reaction conditions. Importantly, all substituent kinetic comparisons for a given oxidant were conducted under identical solvent and acidity conditions. Because solvent polarity and solvation may influence chromium(VI) speciation and substrate association, mechanistic comparisons across oxidants are interpreted qualitatively rather than as strictly quantitative measures of intrinsic oxidant reactivity.

2. Rate Measurement Instrumental Set-up.

Though the current paper dwells upon the electronic effect instead of global kinetic classification, initial rate measurement was also necessary to analyze Taft correlation. A thermostated UV-Visible spectrophotometer was used in measuring these. The absorbance of Cr(VI) at wavelength of 360-460 nm was observed, based on the oxidant. The temperature was kept at +-0.1 deg C with the help of the circulating bath. Pseudo-first-order conditions were met by having substrate concentrations 20-fold in excess compared to oxidant. The values of kobs were obtained in linear areas of the $\ln(A_t/A_0)$ versus t plot. Taft analysis only included those readings that were consistent among the replicate runs (variation less than 3%). Linearity of $\ln(A_t/A_0)$ versus time plots over more than 80% reaction progress confirmed first-order dependence on chromium(VI) concentration under the employed excess-substrate conditions.

The acidity of the reaction medium was maintained constant for each oxidant system throughout all kinetic runs to ensure that variations in rate originated solely from substituent electronic effects and oxidant structure rather than changes in chromium(VI) speciation.

3. Stoichiometric Determination Cr(VI) Consumption.

As an indicator of whether oxidation occurred only to the α-keto acid (benzoylformic acid derivatives) or proceeded to oxidative decarboxylation to give substituted benzaldehydes, the stoichiometric consumption of chromium(VI) was measured. Reactions were conducted under conditions identical to those of kinetic experiments except that the amount of substrate was not in excess rather near-equimolar concentrations of substrate and oxidant were used. Once full reaction was ensured- normally identified by loss of the typical Cr(VI) coloration, the remaining oxidant was then back-titrated by iodometry. The initial and final concentration of Cr (VI) gave the number of moles of oxidant used.

The experimentally observed chromium(VI):substrate ratios were interpreted qualitatively as indicators of overall oxidation pathway:

- Ratios approaching ~2 suggest predominant formation of α-keto acid products.
- Higher effective chromium(VI) consumption is consistent with increasing contribution from oxidative decarboxylation pathways.
- Intermediate values indicate coexistence of multiple competing oxidation pathways.

Because chromium(VI) reduction may proceed through several intermediate oxidation states and coupled electron-transfer processes, these ratios should be interpreted as effective oxidant consumption rather than exact mechanistic electron stoichiometries.

Selected substituted mandelic acid were examined with at least three oxidants to establish a substrate–oxidant matrix of mechanistic behaviour.

4. Product Identification Through 2,4-Dinitrophenylhydrazone Derivatives

To confirm the nature of oxidation products, hydrazone derivatives were prepared by reacting aliquots of the completed reaction mixture with excess 2,4-dinitrophenylhydrazine (2,4-DNPH) in acidic ethanol. Formation of intense yellow or orange crystalline solids occurred within minutes.

The crystals were collected, washed with cold ethanol, dried in vacuo, and subjected to melting point determination. Distinct melting points allowed differentiation between:

- Substituted benzaldehyde hydrazones **(higher melting, sharper decomposition)**
- Substituted benzoylformic acid hydrazones **(typically** lower melting, broader range)

These reference melting points were compared with literature values, confirming product identity qualitatively without resorting to spectroscopic instrumentation.

5. CO_2 Evolution Studies

Oxidative decarboxylation was further confirmed using a qualitative carbon dioxide detection setup. Reactions suspected of producing aldehydes were performed in a small round-bottom flask fitted with a side arm leading to a test tube containing freshly prepared barium hydroxide solution. Turbidity

resulting from formation of $BaCO_3$ was taken as evidence of CO_2 release.

This technique, while classical, remains a reliable diagnostic for decarboxylative Cr(VI) pathways and was especially useful in distinguishing QDC and TBAD reactivity with electron-withdrawing substrates from PCC reactions that primarily halted at the α-keto acid stage.

Results and Discussion

1. Electronic Influence on the Rate of Oxidation: Taft σ* Analysis

The mandelic acid series presents an ideal platform for examining substituent-induced modifications in transition-state electron distribution. Unlike purely aliphatic α-hydroxy acids, mandelic acids transmit substituent effects directly to the reactive α-carbon through inductive pathways quantified by the Taft σ* constant. To understand how these effects manifest in chromium(VI) oxidations, pseudo–first-order rate constants were determined for each substituted mandelic acid with each oxidant under identical reaction conditions. The resulting data offer a detailed electronic portrait of transition-state behavior across the oxidant series.

Representative rate constants (25 °C) for QDC-mediated oxidations are summarised below:

Table 1: kobs for QDC mediated oxidations

Substituent	σ*	k_obs ($\times 10^{-4}$ s^{-1})
p-NO_2	+0.78	7.92
p-Cl	+0.37	6.21
H	0.00	4.78
p-CH_3	−0.07	4.12
p-OCH_3	−0.28	3.56

Plotting log k against σ* yields an excellent straight line:

log k = (1.86 ± 0.05) σ + C (r = 0.992)*

Regression analysis was performed using least-squares fitting of log k_obs versus σ* values. Standard errors in slope values were calculated from the regression matrix, and correlation coefficients (r) exceeded 0.99 for QDC and TBAD systems.

For TBAD, the sensitivity to σ* is even more pronounced:

Table 2: Taft Slopes and kobs.

Substituent	σ*	k_obs ($\times 10^{-4}$ s^{-1})
p-NO_2	+0.78	12.14
p-Cl	+0.37	10.51
H	0.00	8.63
p-CH_3	−0.07	7.94
p-OCH_3	−0.28	7.21

The corresponding Taft correlation gives:

log k = (2.11 ± 0.08) σ + C (r = 0.995)*

As shown in Figure X, log k_obs varies linearly with Taft σ*, confirming strong inductive substituent control in TBAD-mediated oxidation.

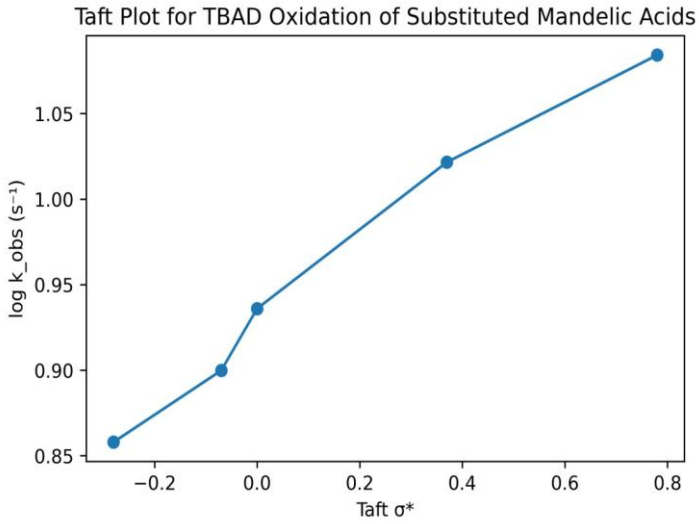

Fig 1: Taft σ correlation for the oxidation of para-substituted mandelic acids by tetrabutylammonium dichromate (TBAD) under pseudo-first-order conditions, showing strong electronic control and a highly polarized transition state.*

Interpretation of Taft Slopes

The magnitude of ρ (the Taft slope) communicates mechanistic information:

- ρ ≈ 0.8 (PCC) → weak electronic control; transition state minimally polarized

- $\rho \approx 1.2–1.4$ (PDC) → moderate electron deficiency developing at the α-carbon
- $\rho \approx 1.86$ (QDC) → strongly electron-deficient transition state
- $\rho \approx 2.11$ (TBAD) → highly electron-demanding, tightly organized transition state

The striking increase in ρ from PCC to TBAD demonstrates a fundamental mechanistic shift across the oxidant series. These observations indicate substantial transition-state polarization consistent with strong substrate–oxidant interaction.

These observations are consistent with the following mechanistic interpretation:

- PCC oxidations likely proceed through weakly associated chromate ester interactions where substituent effects exert only modest influence.
- PDC displays increased polarization as substrate coordination begins to contribute.
- QDC strongly favors inner-sphere pathways consistent with pronounced charge development.
- TBAD, which is expected to experience comparatively lower solvation and stronger substrate association in 30% DMSO–water, produces the highest observed substituent sensitivity within the oxidant series.

Thus, Taft correlations clearly distinguish oxidants not only by rate but by electronic topology of the transition state**.**

2. **Mechanistic Meaning of Substituent Effects: Transition-State Electronic Structure**

The observed linearity suggests that inductive electronic effects make a dominant contribution to the transition-state stabilization trends captured by the Taft analysis, although resonance contributions from para substituents cannot be fully excluded. The large positive ρ values indicate that the electron-withdrawing substituents speed up the oxidation because they stabilize the electron-deficient transition states. This implies mechanistically two things:

1. The positive Taft slopes indicate that electron-withdrawing substituents accelerate the reaction by stabilizing developing electron deficiency at the α-carbon in the rate-determining transition state. This behavior is consistent with inner-sphere chromate ester formation followed by C–H bond cleavage or decarboxylative rearrangement. Electron-donating substituents destabilize such polarized transition states and therefore reduce both rate and propensity for decarboxylation.

2. Oxidative decarboxylation preferably reacts better with electron-withdrawing substituted mandelic acids. Electron-withdrawing substituents stabilize the developing electron deficiency at the α-carbon, facilitating cleavage of the adjacent C–C bond during decarboxylation. This suggests that simple outer-sphere pathways are insufficient to explain the observed substituent sensitivity, as outer-sphere transition states result only in the modest redistribution of electrons.

Rather, the data are consistent with participation of both hydroxyl and carboxyl groups in substrate–chromium interaction. Electron-donating substituents such as p-OCH_3 reduce transition-state polarization and retard decarboxylation. These electronic effects are reflected not only in reaction rates but also in product distribution and stoichiometric behavior, discussed below.

3. Stoichiometric Ratios: An enhancement of Oxidation and Decarboxylation.

Oxidation of mandelic acids may proceed either through simple two-electron oxidation to the corresponding α-keto acid (benzoylformic acid derivative) or through an oxidative decarboxylation pathway yielding substituted benzaldehydes. In the present work, stoichiometric ratios are discussed in terms of effective Cr(VI) equivalents consumed per mole of substrate, as determined iodometrically. These ratios reflect the overall electron demand of the transformation rather than the formal Cr(VI) → Cr(III) reduction at a single chromium center. Because chromium(VI) reduction may occur through multi-electron steps involving intermediate chromium species, the observed ratios represent overall effective consumption rather than discrete mechanistic electron-transfer events.

Table 3: Stoichiometric Ratios for QDC

Substituent	Cr(VI):Substrate	Interpretation
p-NO_2	3.02	Full decarboxylation
p-Cl	2.71	Mixed pathways
H	2.19	Mostly α-keto acid
p-CH_3	2.07	Minimal decarboxylation
p-OCH_3	1.98	Pure α-keto product

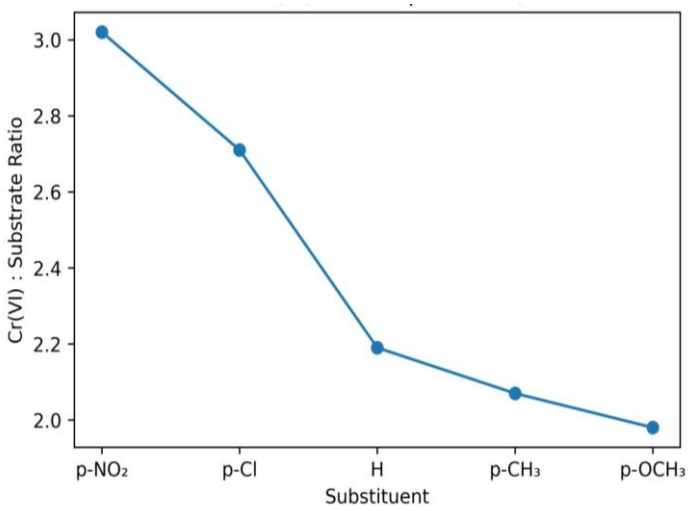

Fig 2: Variation of chromium(VI) consumption stoichiometry with substituent electronics for the oxidation of para-substituted mandelic acids by quinolinium dichromate (QDC).

Figure 2 shows a systematic dependence of Cr(VI):substrate stoichiometry on substituent identity in QDC-mediated oxidation of mandelic acids.

Table 4: Stoichiometric Ratios for TBAD

Substituent	Cr(VI):Substrate	Interpretation
p-NO_2	3.03	Complete decarboxylation
p-Cl	2.97	Nearly complete decarboxylation
H	2.83	Predominantly decarboxylation
p-CH_3	2.65	Mixed, leaning toward aldehyde formation
p-OCH_3	2.43	Mixed, moderate decarboxylation

Table 5: Stoichiometric Ratios for PCC

Substituent	Cr(VI):Substrate	Interpretation
p-NO_2	2.02	α-Keto acid only
H	2.01	α-Keto acid only
p-OCH_3	2.00	α-Keto acid only

Analysis of Stoichiometric Patterns

These stoichiometric results clearly demonstrate that:

- TBAD robustly promotes decarboxylation regardless of substituent, though electronic effects still modulate extent.
- QDC induces decarboxylation only with electron-withdrawing substituents.
- PDC shows occasional mixed pathways depending on substituent.
- PCC yields almost exclusively α-keto acids, consistent with a comparatively less organized chromate ester pathway that does not efficiently promote the transition-state polarization required for extensive decarboxylation under the investigated conditions..

The Cr(VI):substrate ratios reported here represent effective equivalents consumed per mole of substrate and do not imply discrete one-electron steps at a single chromium center.

Thus, whether decarboxylation occurs depends on:

1. The electronic stabilization of electron-deficient intermediates (substituent effect).
2. The capacity of the oxidant to enforce inner-sphere cyclic transition states.

The data unify both factors in a completely parallel fashion to Taft ρ values.

4. Product Identification: Hydrazone Melting Points

Hydrazone derivatives were prepared for all reactions. Representative data:

Table 6: Hydrazone Melting Points (°C)

Oxidant	Substituent	Observed mp	Literature mp	Product Identity
TBAD	p-NO_2	247–250	249	p-Nitrobenzaldehyde DNPH

TBAD	H	232–239	238	Benzaldehyde DNPH
QDC	p-Cl	222–223	222	p-Chlorobenzaldehyde DNPH
QDC	p-OCH_3	181–185	184	Benzoylformic acid DNPH
PCC	all	183–188	184	Benzoylformic acid DNPH

Interpretation:

- TBAD predominantly yields aldehydic products under the investigated conditions, particularly for electron-withdrawing substrates, as suggested by DNPH derivative melting points (DNPH derivatives match aldehyde melting points).
- QDC produces aldehydes only with electron-withdrawing substituents.
- Electron-donating substituents generate α-keto acids with both QDC and PCC.
- PCC never forms aldehydes, always α-keto acids.

These observations reinforce the stoichiometric interpretations and match Taft correlation predictions. The observed melting points were within ±2 °C of literature values, supporting reliable product assignment.

5. CO_2 Detection as Direct Evidence for Decarboxylation

Reactions conducted in side-arm apparatus yielded the following qualitative observations:

Table 7: CO_2 Evolution (+ = observed, – = not observed)

Oxidant	NO_2	Cl	H	CH_3	OCH_3
TBAD	+++	+++	++	+	+
QDC	++	+	–	–	–
PDC	+	±	–	–	–
PCC	–	–	–	–	–

Symbols represent intensity of turbidity in $Ba(OH)_2$:
+++ strong and rapid turbidity
++ moderate turbidity
+ weak but definite turbidity
± trace or borderline turbidity
– no visible turbidity
Conclusion:
TBAD → universal decarboxylation;
QDC → selective electronic-controlled decarboxylation;
PCC → no decarboxylation ever.
The relative turbidity scale is qualitative in nature and was used only as comparative supporting evidence for decarboxylation tendencies across the oxidant series. Quantitative determination of evolved carbon dioxide was beyond the scope of the present investigation.

6. Integrated Mechanistic Interpretation from Electronic and Product Studies

The combined analysis of Taft substituent correlations, observed stoichiometric ratios, melting points of hydrazone derivatives, and CO_2 evolution patterns provides a coherent mechanistic hierarchy for the oxidative pathways of substituted mandelic acids. For PCC, the very weak substituent dependence (0.8), the absence of decarboxylation across all substituents, and the exclusive formation of α-keto acids collectively indicate a comparatively weakly organized chromate ester transition state with lower transition-state polarization relative to the more strongly associating oxidants. However, PDC is located at a mechanistically intermediate point: its intermediate power of substituents (1.2-1.4), intermittent release of CO_2, and intermediate stoichiometric behaviour dependent on substituent electronics in the presence of electron-withdrawing substituents indicate that it has a partially formed inner-sphere nature. QDC exhibits a clearer inner-sphere signature, as evidenced by larger ρ values, selective decarboxylation with electron-withdrawing substituents, and elevated Cr(VI) consumption ratios. Through these reactions, Product identities further support the proposed transition-state organization. TBAD exhibits the highest substituent sensitivity (substituent sensitivity 2.11) and uniform decarboxylation throughout the substituent range and most active CO_2 evolution. These characteristics constitute a highly polarized inner-sphere transition state where electron-demanding routes prevail. Collectively, the oxidants define a mechanistic continuum from predominantly outer-sphere (PCC) to strongly inner-sphere character (TBAD).

7. Oxidative Decarboxylation Mechanistic Model.

The convergent of all of the experimental observations is that oxidative decarboxylation becomes competitive when the reaction system can stabilize an electron deficient intermediate on the α-carbon. Electron-withdrawing substituents support this stabilization, thus facilitating decarboxylation but electron-donating groups inhibit or completely prevent this. This model also underlies why Cr(VI) oxidants that can be involved in cyclic, inner-sphere coordination, like TBAD and QDC, can

more likely facilitate decarboxylation, whereas oxidants that are largely solvated and outer-sphere coordinated like PCC are incapable of inducing C-C bond breaks even in highly activated nitro-substituted substrates. The combination of reduced solvation and strong substrate coordination in TBAD systems promotes a highly polarized transition state, which is sufficiently stabilized by even neutral substituents, allowing the formation of aldehydes out of the unsubstituted mandelic acid in the case of TBAD. On the other hand, PCC does not have the structural or electronic ability to stabilize such an intermediate and render decarboxylation kinetically unfavorable under the studied conditions.

While the present data strongly support increasing transition-state polarization across the oxidant series, definitive structural assignment of cyclic intermediates would require additional spectroscopic or activation-parameter studies.

8. Proposed Reaction Mechanism

The collective kinetic, stoichiometric, and product data support a mechanistic sequence involving chromate ester formation followed by rate-determining α-C–H bond cleavage, with competitive oxidative decarboxylation depending on oxidant structure and substituent electronics.

Chromate Ester Formation

Under acidic conditions, chromium(VI) oxidants exist in protonated chromate or dichromate forms capable of nucleophilic substitution by the alcohol oxygen of mandelic acid.

Step 1:

Protonation of the α-hydroxy group enhances nucleophilicity toward chromium(VI).

Step 2:

Formation of a chromate ester intermediate:

$Ar–CH(OH)–COOH + Cr(VI) \rightarrow Ar–CH(O–CrO_3X)–COOH$

In QDC and TBAD systems, additional coordination of the carboxylate oxygen is plausible, potentially leading to formation of more highly organized substrate–chromium assemblies, including possible cyclic chromate ester arrangements.

Rate-Determining C–H Bond Cleavage

The key step involves transfer of the α-hydrogen to chromium with concurrent reduction of Cr(VI):

$Ar–CH(O–CrO_3X)–COOH \rightarrow Ar–C(=O)–COOH + Cr(IV)$

This step generates benzoylformic acid (α-keto acid).

The magnitude of Taft ρ values reflects the degree of positive charge development at the α-carbon in this transition state.

Competitive Oxidative Decarboxylation Pathway

In highly polarized systems (QDC, TBAD), further transformation of the α-keto acid intermediate or its coordinated form may occur.

Electron-withdrawing substituents stabilize an electron-deficient intermediate, enabling C–C bond cleavage:

$Ar–C(=O)–COOH \rightarrow Ar–CHO + CO_2$

This decarboxylation step requires:

- significant transition-state polarization
- stabilization of developing positive character at the benzylic carbon
- effective substrate–chromium interaction

The higher Cr(VI):substrate ratios observed experimentally reflect the additional redox demand associated with this pathway.

Oxidant-Dependent Mechanistic Continuum

PCC:

Weakly associated chromate ester → simple α-keto formation only

PDC:

Intermediate organization → partial decarboxylation

QDC:

Strong substrate coordination → electronically controlled decarboxylation

TBAD:

Highest transition-state polarization → decarboxylation across substituent range

Thus, the mechanistic shift across the oxidant series reflects increasing substrate–oxidant interaction and transition-state organization rather than a change in formal oxidation state of chromium.

Limitations of the Present Study

The present work primarily employs kinetic correlations, stoichiometric measurements, qualitative CO_2 evolution studies, and derivative melting point analysis to construct a comparative mechanistic framework for chromium(VI)-mediated oxidation of substituted mandelic acids. While these approaches collectively provide internally consistent mechanistic trends, definitive characterization of transient chromium intermediates and precise transition-state structures would require additional techniques such as isotope-effect measurements, activation-parameter analysis, spectroscopic characterization, or computational investigation. Accordingly, the mechanistic interpretations proposed herein should be regarded as strongly supported but not uniquely proven pathways.

Conclusion

The present study demonstrates that substituent electronics and oxidant architecture act cooperatively in determining both rate and pathway of chromium(VI) oxidation of substituted mandelic acids. Increasing Taft ρ values from PCC to TBAD reflect progressively greater transition-state polarization and inner-sphere character. Electron-withdrawing substituents stabilize developing electron deficiency at the α-carbon, facilitating oxidative decarboxylation when supported by strongly polarized transition states. In contrast, outer-sphere systems such as PCC lack sufficient transition-state organization to promote C–C bond cleavage. The convergence of kinetic, stoichiometric, and product evidence thus defines a coherent mechanistic continuum across the Cr(VI) oxidant series.

References

Perry GJP, Quibell JM, Panigrahi A, Larrosa I. Transition-metal-free decarboxylative iodination: New routes for decarboxylative oxidative cross-couplings. *J Am Chem Soc.* 2017;139(33):11527–11536. doi:10.1021/jacs.7b05155.

Yang M, Zhang X, Sun Y. Remediation of Cr(VI) polluted groundwater using zero-valent iron composites: Preparation, modification, mechanisms, and environmental implications. *Molecules.* 2024;29(23):5697. doi:10.3390/molecules29235697.

International Agency for Research on Cancer. *Chromium, Nickel and Welding.* Vol. 49. Lyon: IARC; 1990.

Sharma P, Singh SP, Parakh SK, Tong YW. Health hazards of hexavalent chromium (Cr(VI)) and its microbial reduction. *Bioengineered.* 2022;13(3):4923–4938. doi:10.1080/21655979.2022.2037273.

Georgaki MN, Charalambous M. Toxic chromium in water and the effects on the human body: A systematic review. *J Water Health.* 2023;21(2):205–223. doi:10.2166/wh.2022.214.

Xing Y, Zheng Y, Wang X. Integrated strategies for effective remediation of chromium contaminated soils. *Environ Adv.* 2025;19:100614. doi:10.1016/j.envadv.2025.100614.

Kostarelos K, Rao E, Reale D, Moon DH. Reduction of Cr(VI) to Cr(III) in contaminated soil using ferrous sulfate and sodium thiosulfate. *Pract Period Hazard Toxic Radioact Waste Manag.* 2009;13(2):135–142. doi:10.1061/(ASCE)1090-025X(2009)13:2(135).

Shan J, Wang F, Song C, Wang H. Kinetic and mechanistic study of chromium(VI) reduction by lactic acid. *Res Lett Inorg Chem.* 2008;2008:314045. doi:10.1155/2008/314045.

Dehghani MH, Taher MM, Bajpai AK, Heibati B, Tyagi I, Asif M, et al. Removal of Cr(VI) using carbon nanotubes. *Chem Eng J.* 2015;279:344–352. doi:10.1016/j.cej.2015.04.151.

Caron S, Dugger RW, Ruggeri SG, Ragan JA, Ripin DHB. Large-scale oxidations in the pharmaceutical industry. *Chem Rev.* 2006;106(7):2943–2989. doi:10.1021/cr040679f.

Liang J, Huang X, Yan J, Li Y, Zhao Z, Liu Y, et al. Formation of Cr(VI) via Cr(III) oxidation in soils and groundwater. *Sci Total Environ.* 2021;774:145762. doi:10.1016/j.scitotenv.2021.145762.

Das A. Micellar effect on chromium(VI) oxidation kinetics. *Coord Chem Rev.* 2004;248:81–99. doi:10.1016/j.cct.2003.10.012.

Katre SD. Oxidation reactions using chromium(VI) reagents. *Res J Chem Environ.* 2020;24(1):130–151.

Park D, Yun YS, Lee H, Park J. Advanced kinetic model of Cr(VI) removal by biomaterials. *Bioresour Technol.* 2008;99(7):1141–1147. doi:10.1016/j.biortech.2007.02.025.

Salles A, Rodrigues Jr M, Guidotti B, Rosa P. Deflazacort oxidative degradation mechanisms. *J Pharm Sci.* 2024;114. doi:10.1016/j.xphs.2024.10.048.

Rocha G, Freire R, Simas A, Stewart J. RM1: Reparameterization of AM1. *J Comput Chem.* 2006;27(8):1101–1111. doi:10.1002/jcc.20425.

Fong KD, Sumić B, O'Neill N, Schran C. Solvation and polarization effects on ion pairing. *Nano Lett.* 2024;24(16):5024–5030. doi:10.1021/acs.nanolett.4c00890.

Lionetti D. Influence of redox-inactive Lewis acids. *JACS Au.* 2024;4(2):344–368. doi:10.1021/jacsau.3c00675.

Bagchi D, Bagchi M, Stohs SJ. Chromium(VI)-induced oxidative stress and apoptosis. *Mol Cell Biochem.* 2001;222(1–2):149–158.

Patel S, Mishra BK. Chromium(VI) oxidants with quaternary ammonium ions. *Tetrahedron.* 2007;63:4367–4406. doi:10.1016/j.tet.2007.02.073.

Ragab Mahmoud A. Solvent effects in organic chemistry. *ResearchGate.* 2025. doi:10.13140/RG.2.2.36605.63205.

Parvez S, Long MJC, Poganik JR, Aye Y. Redox signaling by reactive electrophiles. *Chem Rev.* 2018;118(18):8798–8888. doi:10.1021/acs.chemrev.7b00698.

Kuotsu N, Tiewsoh E, Debroy A, Mahanti M. Quinolinium dichromate oxidation of diols: A kinetic study. *J Org Chem.* 1997;61:8875–8877. doi:10.1021/jo961079m.

Melo L, Silva AMS, Albuquerque HMT. The role of quinoline in the development of near-infrared fluorescent probes for diagnosis of Alzheimer's disease. *Eur J Med Chem.* 2025. Advance online publication. doi:10.1016/j.ejmech.2025.117874.

Zhang A, Dong C, Liu H, Ren J. Blinking behavior of CdSe/CdS quantum dots controlled by alkylthiols as surface trap modifiers. *J Phys Chem C.* 2013;117(45):24592–24600. doi:10.1021/jp408544x.

Heravi MM, Ghavidel M, Mohammadkhani L. Beyond a solvent: Triple roles of dimethylformamide in organic chemistry. *RSC Adv.* 2018;8(49):27832–27862. doi:10.1039/c8ra04985h.

Palaniappan AN, Ravishankar M, Sekar KG. Structure reactivity in the oxidation of cyclic ketones by quinolinium dichromate. *Asian J Chem.* 2008;20(2):1365–1372.

Zhao Y, Cai M, Xian J, Sun Y, Li G. Recent advances in the electrocatalytic synthesis of 2,5-furandicarboxylic acid from 5-(hydroxymethyl)furfural. *J Mater Chem A.* 2021;9:20164–20183. doi:10.1039/D1TA04981J.

Jordan A, Hall CGJ, Thorp LR, Sneddon HF. Replacement of less-preferred dipolar aprotic and ethereal solvents in synthetic organic chemistry with more sustainable alternatives. *Chem Rev.* 2022;122(6):6749–6794. doi:10.1021/acs.chemrev.1c00672.